AD-Vol. 61

CONTROL OF VIBRATION AND NOISE: NEW MILLENNIUM

presented at

THE 2000 ASME INTERNATIONAL MECHANICAL ENGINEERING CONGRESS AND EXPOSITION
NOVEMBER 5–10, 2000
ORLANDO, FLORIDA

sponsored by

THE AEROSPACE DIVISION, ASME
THE APPLIED MECHANICS DIVISION, ASME
THE DESIGN ENGINEERING DIVISION, ASME
THE DYNAMIC SYSTEMS AND CONTROL DIVISION, ASME

edited by

HORN-SEN TZOU
UNIVERSITY OF KENTUCKY

M. FARID GOLNARAGHI
UNIVERSITY OF WATERLOO

CLARK J. RADCLIFFE
MICHIGAN STATE UNIVERSITY

THE AMERICAN SOCIETY OF MECHANICAL ENGINEERS
Three Park Avenue / New York, N.Y. 10016

THE QUADRATICALLY-DAMPED MATHIEU EQUATION AND ITS APPLICATION TO SUBMARINE DYNAMICS

Richard H. Rand
Dept. of Theoretical & Applied Mechanics
Cornell University, Ithaca, NY 14853
email:rhr2@cornell.edu

Deepak V. Ramani
Dept. of Theoretical & Applied Mechanics
Cornell University, Ithaca, NY 14853
email:dvr3@cornell.edu

William L. Keith
Naval Undersea Warfare Center
Newport RI 02841
email:wlkeith@hotmail.com

Kimberly M. Cipolla
Naval Undersea Warfare Center
Newport RI 02841
email:cipollakm@npt.nuwc.navy.mil

ABSTRACT

This work is motivated by naval use of passive towed sonar arrays of hydrophones. We consider the simplest model of a towed mass. The mass is considered to move only in a horizontal direction x perpendicular to the tow direction. The tension in the tow cable is expected to be nonconstant due to turbulence, and is modeled by a sinusoidal forcing function. The resulting differential equations are analyzed for linear stability and nonlinear dynamical effects. In particular we study the nonlinear dynamics of the ODE:

$$\ddot{x} + (\delta + \epsilon \cos t)x + \dot{x}|\dot{x}| = 0$$

INTRODUCTION

Passive towed arrays are one of the primary acoustic sensors used by submarines. The position of a towed array relative to the towing submarine is determined by a variety of factors, including such things as the ship's speed, tow cable length and composition, and array buoyancy. The deployment and control of a line must be done in a complex, unsteady ocean environment which is complicated by the turbulent flows associated with the towing vessel and the flow past the line itself. Movement of the line may be accomplished through the use of small lifting devices, referred to as 'lateral force devices' or LFDs.

The dynamics of an LFD are complicated by changes in the tow line tension due to flow-induced vibration caused by coherent turbulent structures. These structures result from the turbulent boundary layer on the tow line upstream of the LFD and vortex shedding from the tow line due to cross-flow. Full scale experiments in a towing tank have shown that an LFD can exhibit unstable motions under particular conditions (Cipolla et al.,1997). The objective of this work is to provide analytical and numerical modeling of this effect, and to determine parameter ranges in which instabilities will result in undesirable large amplitude motions of the LFD and accompanying temporal variations in the array position.

SIMPLIFIED MODEL

We investigate the properties of a simplified model of a towed LFD. The coordinate x is used to measure the horizontal location of the LFD perpendicular to the tow direction, see Figure 1. We consider two cases: a) in which the tow cable is rigid, and hence can withstand compressive loads, and b) in which the tow cable is incapable of compression. In both cases, the tension T in the tow cable is expected to be nonconstant due to turbulence. In case a), T is modeled by a sinusoidal forcing function, $T = T_0 + T_1 \cos \Omega t$, while in case b) we assume $T = (T_0 + T_1 \cos \Omega t)H(T_0 + T_1 \cos \Omega t)$ where $H(\cdot)$ is the

Heaviside step function. This leads to the approximate differential equation:

$$m\ddot{x} + T\frac{x}{L} + c\dot{x}|\dot{x}| = c_0 U(t)^2 \qquad (1)$$

Here the force exerted by the cable on the LFD is Tx/L. We neglect changes in the length L of the tow cable and treat L as a constant. The LFD is treated as a plate oriented so that a normal to the plate's surface points in the x-direction. The term $c\dot{x}|\dot{x}|$ is a fluid drag force and the term $c_0U(t)^2$ is a fluid lift force. For mathematical simplicity in what follows, we assume that the lift force is negligible, an assumption which is equivalent to assuming that the angle of attack of the plate with respect to the tow direction is zero.

Eq.(1) may be rescaled to take on one of the forms:
Case a) (rigid cable):

$$\ddot{x} + (\delta + \epsilon\cos t)x + \dot{x}|\dot{x}| = 0 \qquad (2)$$

Case b) (flexible cable):

$$\ddot{x} + (\delta + \epsilon\cos t)\ H(\delta + \epsilon\cos t)x + \dot{x}|\dot{x}| = 0 \qquad (3)$$

Eq.(2) is a nonlinear Mathieu equation and Eq.(3) is a nonlinear Hill's equation. In this paper we present a linear stability analysis of both eqs.(2) and (3), and a nonlinear analysis of Eq.(2).

Although eqs.(2) and (3) offer simplified models of the real world situation, they are nevertheless nonlinear differential equations and as such may be expected to support a variety of nonlinear phenomena including instability due to subharmonic resonance and related bifurcations, as well as chaos.

The dynamics of eqs.(2) and (3) are determined by the values of the parameters δ and ϵ. We shall be interested in describing the dynamics of eqs.(2) and (3) in the region of the $\delta-\epsilon$ parameter plane for which $0 < \delta < 1$ and $0 < \epsilon < 3$. This region is chosen because it includes some important dynamical effects, including a well-known instability tongue emerging from the point $\delta = \frac{1}{4}, \epsilon = 0$, which is due to the 2:1 subharmonic resonance in the linear Mathieu equation.

LINEAR STABILITY ANALYSIS

Eq.(2) admits the exact solution $x = 0$. Its stability is governed by the linear Mathieu equation,

$$\ddot{x} + (\delta + \epsilon\cos t)x = 0 \qquad (4)$$

A point (δ, ϵ) is said to be stable if all solutions to the linear equation (4) are bounded, and unstable if an unbounded solution exists. The analysis of Eq.(4) dates back to the nineteenth century. See (Stoker,1950) for an excellent summary. Regions of instability, called tongues, emerge from the points $\delta = N^2/4$, $\epsilon = 0$, where $N = 0, 1, 2, 3, \cdots$. These tongues correspond to resonances between the natural frequency of the pendulum-like motion of the towed LFD and the forcing frequency in the tow line due to turbulence in the flow. For small values of ϵ, which is related to the amplitude of the forcing function, the largest instability occurs for $N = 1$. See Figure 2 in which the $N = 1$ tongue is displayed, as well as part of the $N = 2$ tongue. Although the linear theory predicts that inside these tongues the motion will become unbounded, the nonlinear term in Eq.(2) causes the resonance to detune as the amplitude of x grows. The net effect is the creation of a periodic motion having finite amplitude inside the various tongues, at least for small ϵ.

A similar situation exists for Eq.(3). See Figure 2 which also shows the stability chart for Eq.(3). Note that eqs.(2) and (3) are identical for $|\delta| \leq |\epsilon|$, in which case the tow cable remains in tension for all t.

NONLINEAR ANALYSIS FOR SMALL ϵ

For small values of the parameter ϵ, the method of averaging (see e.g. (Rand,1994)) may be used to obtain approximate expressions for periodic solutions to the nonlinear Eq.(2). In the case of the $N = 1$ tongue, we introduce a detuning parameter δ_1:

$$\delta = \frac{1}{4} + \epsilon\delta_1 \qquad (5)$$

and we assume a solution of the form:

$$x(t) = R\ \cos\left(\frac{t}{2} + \psi\right) \qquad (6)$$

where R and ψ are slowly varying functions of time t. Application of the method of averaging gives the following values for R and ψ which correspond to stable periodic motions:

$$R = \frac{3\pi}{4}\sqrt{1 - 4\delta_1^2}, \qquad \psi = \frac{1}{2}\cos^{-1}(-2\delta_1). \qquad (7)$$

This result, which agrees with numerical integration of Eq.(2), states that there is an attractive period-2 subharmonic motion at all points inside the $N = 1$ tongue (at least for small ϵ.)

The method of averaging can similarly be applied to $N = 2$ tongue. In this case it is necessary to include terms of order ϵ^2. The results state that there are two attractive period-1 motions at all points inside the $N = 2$ tongue, as follows.

In this case, the detuning takes the form

$$\delta = 1 + \epsilon\delta_1 + \epsilon^2\delta_2, \tag{8}$$

and Eq.(2) takes the form

$$\ddot{x}+x = -\epsilon\left(\delta_1 x + x\cos t + \dot{x}^2\mathrm{sgn}\,(\dot{x})\right) - \epsilon^2\delta_2 x \equiv -\epsilon G_1 - \epsilon^2 G_2. \tag{9}$$

For $\epsilon = 0$, equation (9) has the solution

$$x = R\cos(t+\psi) \tag{10}$$
$$\dot{x} = -R\sin(t+\psi). \tag{11}$$

This solution becomes the basis for the variation of parameters, which leads to the slow flow equations

$$\dot{R} = \epsilon G_1 \sin(t+\psi) + \epsilon^2 G_2 \sin(t+\psi) \tag{12}$$
$$R\dot{\psi} = \epsilon G_1 \cos(t+\psi) + \epsilon^2 G_2 \cos(t+\psi). \tag{13}$$

The second order averaging is effected by making a near identity transformation of the form

$$R = a + \epsilon W_1(a,\psi,t) + \epsilon^2 V_1(a,\psi,t) + \cdots \tag{14}$$
$$\psi = \psi + \epsilon W_2(a,\psi,t) + \epsilon^2 V_2(a,\psi,t) + \cdots, \tag{15}$$

where the W_i and V_i are chosen to simplify the resulting equations as much as possible.

In order to simplify the calculation of the W_i, we expand the signum function in a Fourier sine series:

$$\mathrm{sgn}(\sin(t+\psi)) = \frac{4}{\pi}\sum_{n=1}^{\infty}\frac{1}{2n-1}\sin[(2n-1)(t+\psi)]. \tag{16}$$

Using this representation of the signum function and carrying out the averaging, the slow equations are found to be

$$\dot{a} = -\epsilon\tfrac{4a^2}{3\pi} + \epsilon^2\left(\tfrac{-a}{8}\sin 2\psi - \tfrac{a^2\delta_1}{3\pi}\right) \tag{17}$$
$$\dot{\psi} = \epsilon\tfrac{\delta_1}{2} + \epsilon^2\left(-\tfrac{1}{8}\cos 2\psi + \tfrac{\delta_2}{2} - \tfrac{\delta_1^2}{8} - \tfrac{Ka^2}{\pi^2} - \tfrac{1}{12}\right) \tag{18}$$

where K is a constant whose value depends on the order of the truncation of the Fourier series. Numerical experiments indicate that K converges to a value near 1.05261. However, the exact value of K is unimportant as it is a higher order term in the slow flow equations. From equation (17), a is an $O(\epsilon)$ term, thus $\epsilon^2 K a^2$ is an $O(\epsilon^4)$ term, and will be ignored.

Eqs.(17) and (18) have as fixed points

$$a = -\frac{\epsilon\pi}{32}\sqrt{5 + 48\delta_2 - 144\delta_2^2} \tag{19}$$
$$\psi = \frac{1}{2}\cos^{-1}\left[\frac{2}{3}(6\delta_2 - 1)\right]. \tag{20}$$

Note that this represents two fixed points. Unlike in the first order averaging near the $N = 1$ tongue, the amplitude of the limit cycles in this case depend on the value of the parameter ϵ. Numerical simulations show good agreement with the predicted value of the amplitude of the limit cycle in Eq.(19).

A SECONDARY BIFURCATION

Numerical simulation of Eq.(2) shows that as one traverses the right hand boundary C of the $N = 1$ tongue, the change in stability of the $x = 0$ solution (which defines this boundary C) is accompanied by a bifurcation involving the creation of a periodic motion. We define point P on the boundary C to be the point at which the curve C has a vertical tangency. See Fig.3. We find that for points on C below P, a stable period-2 motion is born as we cross C from right to left. However, for points on C above P, an unstable period-2 motion is born as we cross C from left to right. The region of the parameter plane which lies just to the right of C and above P thus contains three steady states: 1) the rest solution $x = 0$, 2) the stable periodic motion which is born as curve C is crossed from right to left below P (and which continues to exist as C is crossed from left to right above P), and 3) the unstable periodic motion which is born as C is crossed from left to right above P. Simulation shows that the stable manifolds of the unstable periodic motion separate those initial conditions which are attracted to the rest solution $x = 0$ from those that are attracted to the stable periodic motion.

In addition to these observations, numerical simulation also shows that there is another bifurcation curve B emanating from point P on which the stable and unstable periodic motions of the preceding paragraph coalesce. On curve B the system exhibits a secondary bifurcation which can be described as a saddle-node of limit cycles.

PERTURBATION ANALYSIS AT POINT P

We use a perturbation method to demonstrate that at point P the transition curve changes from a supercritical bifurcation curve to a subcritical bifurcation curve. We begin by introducing a small parameter μ into Eq.(2) by replacing x by μx, giving:

$$\ddot{x} + (\delta + \epsilon \cos t)x + \mu \dot{x}|\dot{x}| = 0 \tag{21}$$

Then we expand x and δ in power series, and we define a quantity ϵ_1 which measures how far we are from point P:

$$x = x_0 + \mu x_1 + \mu^2 x_2 + \mu^3 x_3 + \mu^4 x_4 + \cdots \tag{22}$$
$$\delta = \delta_0 + \mu\delta_1 + \mu^2\delta_2 + \mu^3\delta^3 + \mu^4\delta_4 + \cdots \tag{23}$$
$$\epsilon = \epsilon_0 + \mu\epsilon_1, \tag{24}$$

Here δ_0 and ϵ_0 correspond to point P. Note that we are perturbing off of the linear Mathieu eq.(4), i.e. the unperturbed solution will involve Mathieu functions (Abramowitz and Stegun, 1965), in contrast to the usual sines and cosines. We shall require that each of the functions $x_i(t)$ be periodic.

With these expansions, the perturbation equations then become

$$Lx_0 = 0 \tag{25}$$
$$Lx_1 = -\delta_1 x_0 - \epsilon_1 x_0 \cos t - \frac{dx_0}{dt}\left|\frac{dx_0}{dt}\right| \tag{26}$$
$$Lx_2 = -\delta_2 x_0 - \delta_1 x_1 - \epsilon_1 x_1 \cos t - 2\frac{dx_1}{dt}\left|\frac{dx_0}{dt}\right| \tag{27}$$
$$Lx_3 = -\delta_3 x_0 - \delta_2 x_1 - \delta_1 x_2 - \epsilon_1 x_2 \cos t - 2\frac{dx_2}{dt}\left|\frac{dx_0}{dt}\right| - \operatorname{sgn}\left[\frac{dx_0}{dt}\right]\left(\frac{dx_1}{dt}\right)^2 \tag{28}$$
$$Lx_4 = -\delta_4 x_0 - \delta_3 x_1 - \delta_2 x_2 - \delta_1 x_3 - \epsilon_1 x_3 \cos t - 2\frac{dx_3}{dt}\left|\frac{dx_0}{dt}\right| - 2\operatorname{sgn}\left[\frac{dx_0}{dt}\right]\frac{dx_1}{dt}\frac{dx_2}{dt} - \frac{1}{3}\left(\frac{dx_1}{dt}\right)^3 \delta\left(\frac{dx_0}{dt}\right), \tag{29}$$

where the operator L is defined to be the Mathieu operator

$$L \equiv \frac{d^2}{dt^2} + (\delta_0 + \epsilon_0)\cos t. \tag{30}$$

Because point P lies on the right-hand transition curve of the N=1 tongue, any periodic solution of Eq.(25) must be an odd periodic function (Stoker,1950). We denote this solution by

$$x_0 = Af_1. \tag{31}$$

Here $f_1(t)$ is a periodic solution of Mathieu's eq.(4) and is called a Mathieu function (Abramowitz and Stegun, 1965). We introduce the notational convention that any function labelled f_i is an odd function, whereas any function labelled g_i is an even function.

We proceed to find x_1 by substituting Eq.(31) into Eq.(26) and choosing δ_1 to eliminate secular terms. The secular terms are eliminated by using the Fredholm alternative theorem which states that for a periodic solution to exist for

$$Lx = F, \tag{32}$$

the function F must be orthogonal to the null space of the adjoint operator L^*. In this case, L is self-adjoint, and its nullspace is spanned by the function f_1. The orthogonality condition is expressed as

$$\int_0^{4\pi} f_1 F \, dt = 0. \tag{33}$$

Carrying out the substitution, the Fredholm condition then becomes

$$A\delta_1 \int_0^{4\pi} f_1^2 \, dt + A\epsilon_1 \int_0^{4\pi} f_1^2 \cos t \, dt + A^2 \int_0^{4\pi} f_1 \dot{f}_1 \left|\dot{f}_1\right| \, dt = 0. \tag{34}$$

The third term in Eq.(34) vanishes because f_1 is odd and therefore its derivative is even, which makes the integrand odd, and the integral of an odd function over a single period is zero. The Fredholm condition thus simplifies to

$$\frac{\epsilon_1}{\delta_1} = \frac{\int_0^{4\pi} f_1^2 \, dt}{\int_0^{4\pi} f_1^2 \cos t \, dt}. \tag{35}$$

Since the nonlinear terms in Eq.(26) do not enter into Eq.(35), the latter equation refers to the linear Mathieu eq.(4) as well as to Eq.(21). Thus the quantity ϵ_1/δ_1 represents the local slope of the transition curve of the linear Mathieu eq.(4) near the point (δ_0, ϵ_0). Because point P corresponds to a vertical tangency of the transition curve, Eq.(35) yields the following two conditions

$$\delta_1 = 0 \tag{36}$$

$$\int_0^{4\pi} f_1^2 \cos t \, dt = 0. \tag{37}$$

Taking $\delta_1 = 0$, Eq.(26) becomes

$$Lx_1 = -A\epsilon_1 f_1 \cos t - A^2 \dot{f}_1 \left|\dot{f}_1\right|. \tag{38}$$

The first of the nonhomogeneities in Eq.(38) is odd, while the second is even. Due to linearity we can consider each of these terms individually. The odd term will give rise to an odd solution, whereas the even term will give rise to an even solution. The solution for x_1 can then be written

$$x_1 = A\epsilon_1 f_2 + A^2 g_1, \tag{39}$$

where

$$Lf_2 = -f_1 \cos t \tag{40}$$

$$Lg_1 = -\dot{f}_1 \left|\dot{f}_1\right|. \tag{41}$$

While we have omitted the details, it is possible to show by a direct computation that the results we obtain are invariant under addition of an arbitrary multiple of the homogeneous solution, f_1. Therefore, we have chosen not to include any explicit multiple of f_1 (the complementary solution.)

In similar fashion, the second Fredholm condition, arising from Eq. (27), is

$$\delta_2 \int_0^{4\pi} f_1^2 \, dt + \epsilon_1^2 \int_0^{4\pi} f_1 f_2 \cos t \, dt + 2A^2 \int_0^{4\pi} f_1 g_1 \left|\dot{f}_1\right| \, dt = 0. \tag{42}$$

Solving this for δ_2 we obtain,

$$\delta_2 = k_1 \epsilon_1^2 + 2k_2 A^2, \tag{43}$$

where we have defined

$$k_1 \equiv -\frac{\int_0^{4\pi} f_1 f_2 \cos t \, dt}{\int_0^{4\pi} f_1^2 \, dt} \tag{44}$$

$$k_2 \equiv -\frac{\int_0^{4\pi} f_1 g_1 \left|\dot{f}_1\right| \, dt}{\int_0^{4\pi} f_1^2 \, dt}. \tag{45}$$

This procedure is repeated for succeeding orders of the perturbation analysis. At each stage, the latest δ_i is obtained from the Fredholm condition. Using this value the differential equation for x_i is solved. At each stage, new constants k_i are introduced. Because the δ_i and the k_i determine the nature of the bifurcation at point P, we give their values here. The definitions of the f_i and the g_i along with the solution to Eqs. (25) – (28) are given in the Appendix.

The δ_i are obtained as

$$\delta_1 = 0 \tag{46}$$

$$\delta_2 = k_1 \epsilon_1^2 + 2k_2 A^2 \tag{47}$$

$$\delta_3 = k_3 \epsilon_1^2 + k_4 A^2 \epsilon_1 \tag{48}$$

$$\delta_4 = k_5 A^4 + k_6 A^2 \epsilon_1^2 + k_7 \epsilon_1^4, \tag{49}$$

where

$$k_1 = -\frac{\int_0^{4\pi} f_1 f_2 \cos t \, dt}{\int_0^{4\pi} f_1^2 \, dt} \tag{50}$$

$$k_2 = -\frac{\int_0^{4\pi} f_1 g_1 \left|\dot{f}_1\right| \, dt}{\int_0^{4\pi} f_1^2 \, dt} \tag{51}$$

$$k_3 = -\frac{\int_0^{4\pi} k_1 f_1 f_2 + f_1 f_2 \cos t \, dt}{\int_0^{4\pi} f_1^2 \, dt} \tag{52}$$

$$k_4 = -\frac{\int_0^{4\pi} 2k_2 f_1 f_2 + 2 f_1 f_4 \cos t + 2 f_1 g_2 \left|\dot{f}_1\right| \, dt}{\int_0^{4\pi} f_1^2 \, dt} - \frac{\int_0^{4\pi} 2 f_1 \dot{f}_2 g_1 \operatorname{sgn} \dot{f}_1 \, dt}{\int_0^{4\pi} f_1^2 \, dt} \tag{53}$$

$$k_5 = -\frac{\int_0^{4\pi} 4 f_1 \dot{f}_4 g_1 \operatorname{sgn} \dot{f}_1 + 2 f_1 g_4 \left|\dot{f}_1\right| \, dt}{\int_0^{4\pi} f_1^2 \, dt} \tag{54}$$

$$k_6 = -\frac{\int_0^{4\pi} 2 f_1 \dot{f}_3 g_1 \operatorname{sgn} \dot{f}_1 + 2 f_1 \dot{f}_2 g_2 \operatorname{sgn} \dot{f}_1 \, dt}{\int_0^{4\pi} f_1^2 \, dt} - \frac{\int_0^{4\pi} 2 f_1 g_3 \left|\dot{f}_1\right| + 2k_1 f_1 f_4 + 2k_2 f_1 f_3 \, dt}{\int_0^{4\pi} f_1^2 \, dt} - \frac{\int_0^{4\pi} k_4 f_1 f_2 + f_1 f_5 \cos t \, dt}{\int_0^{4\pi} f_1^2 \, dt} \tag{55}$$

$$k_7 = -\frac{\int_0^{4\pi} k_1 f_1 f_3 + f_1 f_g \cos t + k_3 f_1 f_2 \, dt}{\int_0^{4\pi} f_1^2 \, dt}. \quad (56)$$

Reconstruction of δ gives a relationship between δ, ϵ_1, and A:

$$\Delta \equiv \delta - \delta_0 = k_1\epsilon_1^2 + k_3\epsilon_1^3 + k_7\epsilon_1^4 + A^2\left(2k_2 + k_4\epsilon_1 + k_6\epsilon_1^2\right) + A^4 k_5. \quad (57)$$

The goal is to obtain a value of A for periodic motions given a specific value of δ and ϵ. Since $A = 0$ corresponds to the linear Mathieu eq.(4), setting $A = 0$ in Eq.(57) gives an expression for the transition curve in the linear Mathieu eq. near point P. With this as motivation, we define new variables u and v so that $u = 0$ is the transition curve, and the origin of the new coordinate system is the point P:

$$u = \Delta - k_1\epsilon_1^2 - k_3\epsilon_1^3 - k_7\epsilon_1^4 \quad (58)$$

$$v = \epsilon_1. \quad (59)$$

In these variables, Eq. (57) becomes

$$u = A^2\left(2k_2 + k_4 v + k_6 v^2\right) + A^4 k_5. \quad (60)$$

We consider v small, and therefore neglect higher order terms in v. Numerical simulation has shown that $k_4 \approx 0.075$ and $k_2 \approx k_5 \approx 0.00044$, so that Eq. (60) can be approximately written:

$$u = A^2 k_4 v. \quad (61)$$

For periodic motions to be born, A must be real. If $v < 0$ then $u < 0$. Therefore, below point P, periodic motions are born by moving *into the tongue*. Whereas if $v > 0$ then $u > 0$. Thus, above point P, periodic motions are born by moving *out of the tongue*. This situation, along with the full description of all the periodic orbits, is shown in Fig.4. This illustrates that the nature of the bifurcation at the transition curve changes at point P.

Numerical simulation of the system is complicated by the fact that all the f_i and the g_i must be periodic functions. Thus, the initial conditions need to be chosen carefully. A shooting procedure was used to first locate δ_0 and ϵ_0, and then find the initial conditions. From this procedure, we find the following approximate values for δ_0, ϵ_0, and the k_i

$$\delta_0 = 0.630420248517018 \quad (62)$$

$$\epsilon_0 = 1.438618533234412 \quad (63)$$

$$k1 = -0.176795720204350 \quad (64)$$

$$k2 = 0.000449148087856 \quad (65)$$

$$k3 = 0.023845390107660 \quad (66)$$

$$k4 = 0.074924742628499 \quad (67)$$

$$k5 = 0.000442971060543 \quad (68)$$

$$k6 = 0.091716579381791 \quad (69)$$

$$k7 = 0.008726800055536 \quad (70)$$

If we take $\delta = 0.631$, and $\epsilon = 1.47$, we find $u \approx 7.531 \times 10^{-4}$ and $v \approx 0.0314$. This leads to an approximate value of $A = 0.475$. Fig.5 shows a comparison between the approximate periodic motion for these parameters as computed by the perturbation method and the periodic motion found by numerical integration. Since this periodic motion is unstable, it was obtained using numerical integration by adjusting initial conditions to approximately lie on its stable manifold, i.e. to lie on the boundary which separates the two attractors (the origin and the stable periodic motion).

Note that the method has not produced an expression for the secondary bifurcation curve. Current research involves extending the method to include terms of $O(\epsilon^5)$, which we expect will produce the desired approximation.

CHAOS

Numerical simulation of Eq.(2) has also shown that there is a region of the parameter plane which involves a variety of complicated bifurcations including a period-doubling route to chaos. This region is shown in Fig.3. Period-doubling occurs along Curve D, and period-quadrupling occurs along curve Q.

CONCLUSIONS

We have seen that the simplified model of an LFD displays a wide range of dynamical behavior, depending on the values of the associated parameters. For naval applications, it is desirable to eliminate as much of the x oscillation of the LFD as possible. To this end, an attractive strategy would be to operate the LFD in a parameter range for which the rest solution $x = 0$ is linearly stable. Our analysis has shown, however, that, at least in the case of a rigid tow strut, this strategy will not necessarily work due to nonlinear effects. In particular, in the case of Eq.(2), if the parameters are chosen so as to lie above the curve of secondary bifurcation, see Fig.3, then although the rest solution is stable, there also exists a stable periodic motion. With two stable states present, the one which actually occurs depends on the initial conditions. Since in the application to submarines the initial conditions occur at random,

it is impossible to select them so that the desirable $x = 0$ steady state is achieved, even though this state is attractive. It is therefore advisable to avoid such a region of bistability.

We have studied the problem analytically using two perturbation methods. The first, valid for small ϵ, is a standard procedure and showed that there exist periodic motions inside the $N = 1$ and $N = 2$ tongues, born as the tongue regions are entered. The second perturbation method offers a new approach involving perturbing off of Mathieu functions. It showed that above point P periodic motions are born as the $N = 1$ tongue region is exited through its right-hand boundary.

ACKNOWLEDGEMENT

The authors thank Professor T. Wei of Rutgers University for his technical contributions. Partial funding was provided by the Office of Naval Research, Program Officer Dr. Roy C. Elswick, ONR 321, and by NUWC, Code 10, Dr. Richard Nadolink. Author DVR was supported under a National Science Foundation Graduate Fellowship.

REFERENCES

Abramowitz, M. and Stegun, I., *Handbook of Mathematical Functions*, Dover Publications, 1965.

Cipolla, K.M., Keith, W.L., and Norris, R.P., *Passive Control of a Towed Sonar System with Hydrodynamic Lifting Surfaces*, Proceedings of the Third International Symposium on Performance Enhancements for Marine Applications, 5-8 May 1997, Newport RI.

Stoker, J.J., *Nonlinear Vibrations in Mechanical and Electrical Systems*, Wiley, New York, 1950.

Rand, R.H., *Topics in Nonlinear Dynamics with Computer Algebra*, Gordon and Breach Science Publishers, Langhorne, PA, 1994.

APPENDIX

In this appendix we present definitions for the functions in the perturbation method at point P. The method for developing these is given in the text.

$$x_0 = Af_1 \tag{71}$$
$$x_1 = A\epsilon_1 f_2 + A^2 g_1 \tag{72}$$
$$x_2 = A\epsilon_1^2 f_3 + A^2\epsilon_1 g_2 + 2A^3 f_4 \tag{73}$$
$$x_3 = A^2\epsilon_1^2 g_3 + A^4 g_4 + A^3\epsilon_1 f_5 + A\epsilon_1^3 f_6, \tag{74}$$

where

$$Lf_1 = 0 \tag{75}$$
$$Lf_2 = -f_1 \cos t \tag{76}$$
$$Lg_1 = -\left|\dot{f}_1\right| \tag{77}$$
$$Lf_3 = -k_1 f_1 - f_2 \cos t \tag{78}$$
$$Lf_4 = -k_2 f_1 - \dot{g}_1 \left|\dot{f}_1\right| \tag{79}$$
$$Lg_2 = -g_1 \cos t - \dot{f}_2 \left|\dot{f}_1\right| \tag{80}$$
$$Lf_5 = -k_4 f_1 - 2k_2 f_2 - 2f_4 \cos t - 2\dot{g}_2 \left|\dot{f}_1\right| - 2\dot{f}_2 \dot{g}_1 \operatorname{sgn}\dot{f}_1 \tag{81}$$
$$Lf_6 = -k_3 f_1 - k_1 f_2 - f_3 \cos t \tag{82}$$
$$Lg_3 = -k_1 g_1 - g_2 \cos t - 2\dot{f}_3 \left|\dot{f}_1\right| - \dot{f}_2{}^2 \operatorname{sgn}\dot{f}_1 \tag{83}$$
$$Lg_4 = -2k_2 g_1 - 4\dot{f}_4 \left|\dot{f}_1\right| - \dot{g}_1{}^2 \operatorname{sgn}\dot{f}_1 \tag{84}$$

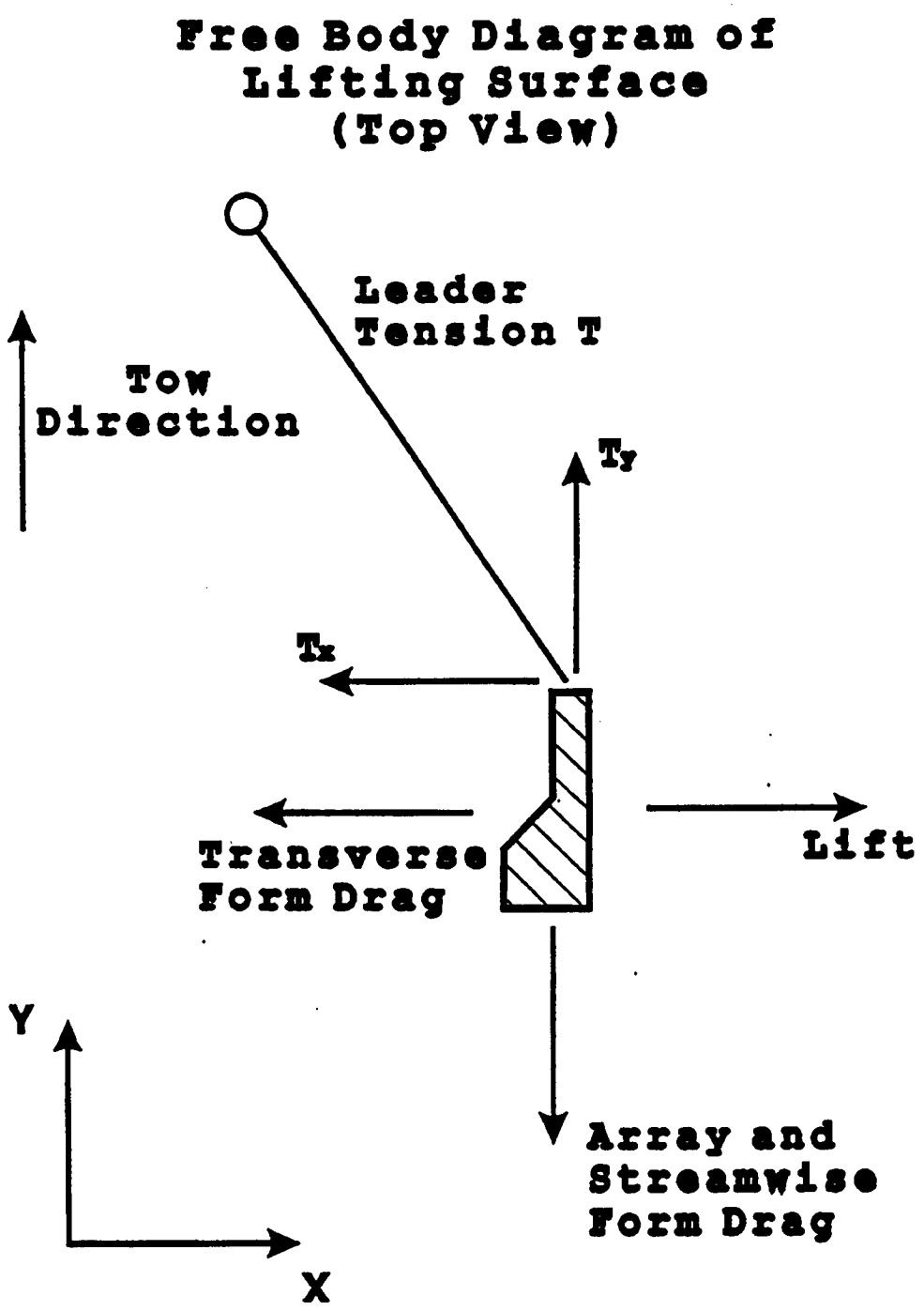

Figure 1. Simplified model of an LFD (lateral force device). The tension in the tow cable is expected to be nonconstant due to turbulence and is modeled by a sinusoidal forcing function. We neglect motion in the y-direction and we treat the cable length L as a constant. The LFD is treated as a plate oriented so that a normal to the plate's surface points in the x-direction. For mathematical simplicity we assume that the lift force is negligible, an assumption which is equivalent to assuming that the angle of attack of the plate with respect to the tow direction is zero.

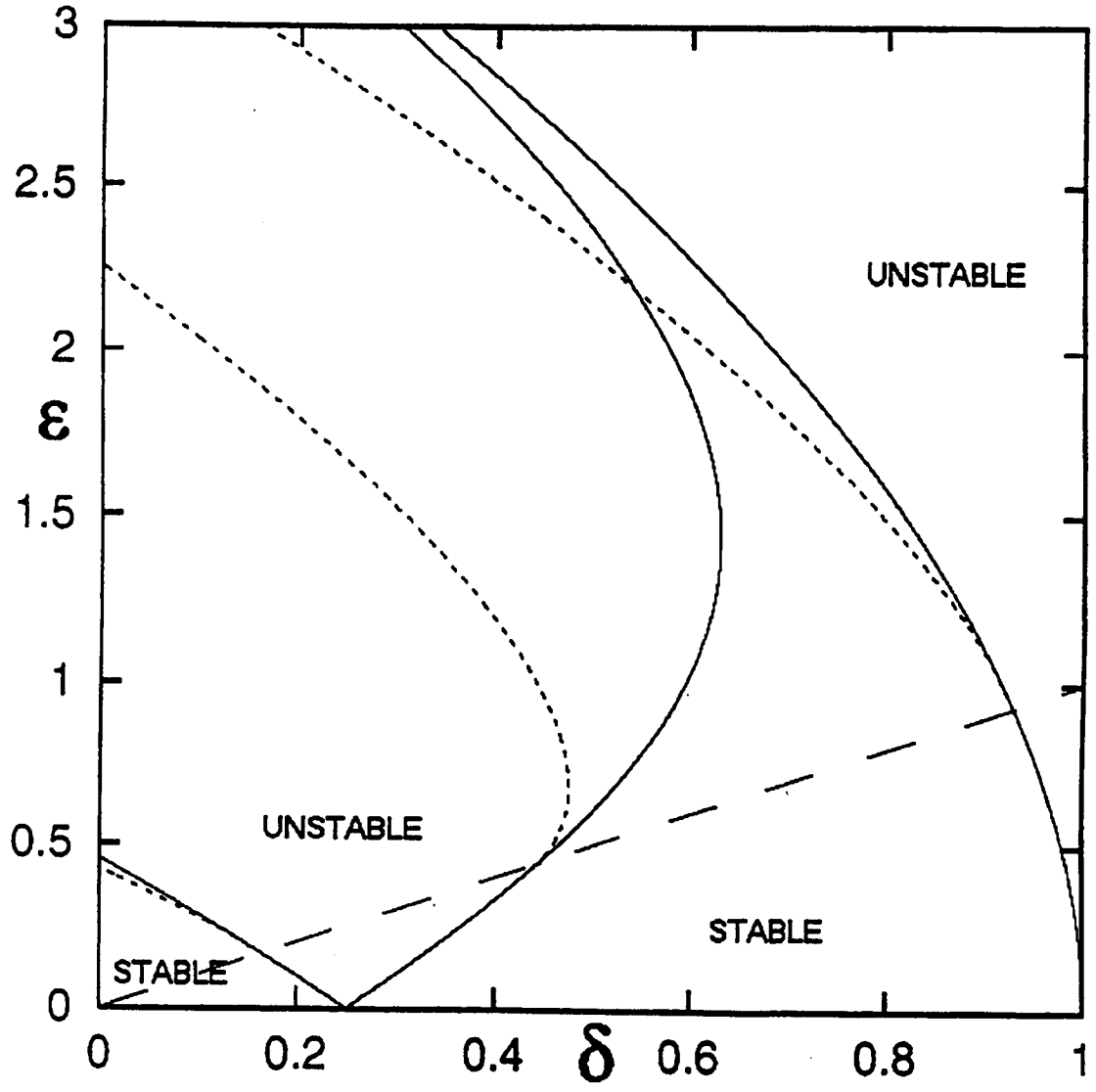

Figure 2. Regions of linear stability and instability in the $\delta - \epsilon$ plane for eq.(2) (solid lines) and eq.(3) (dotted lines). Eq.(3) corresponds to a flexible cable while eq.(2) corresponds to a rigid strut. These equations are identical for points below the straight line $\delta = \epsilon$, which is shown dashed. Points below the dashed line correspond to cases in which the cable remains in tension for all time.

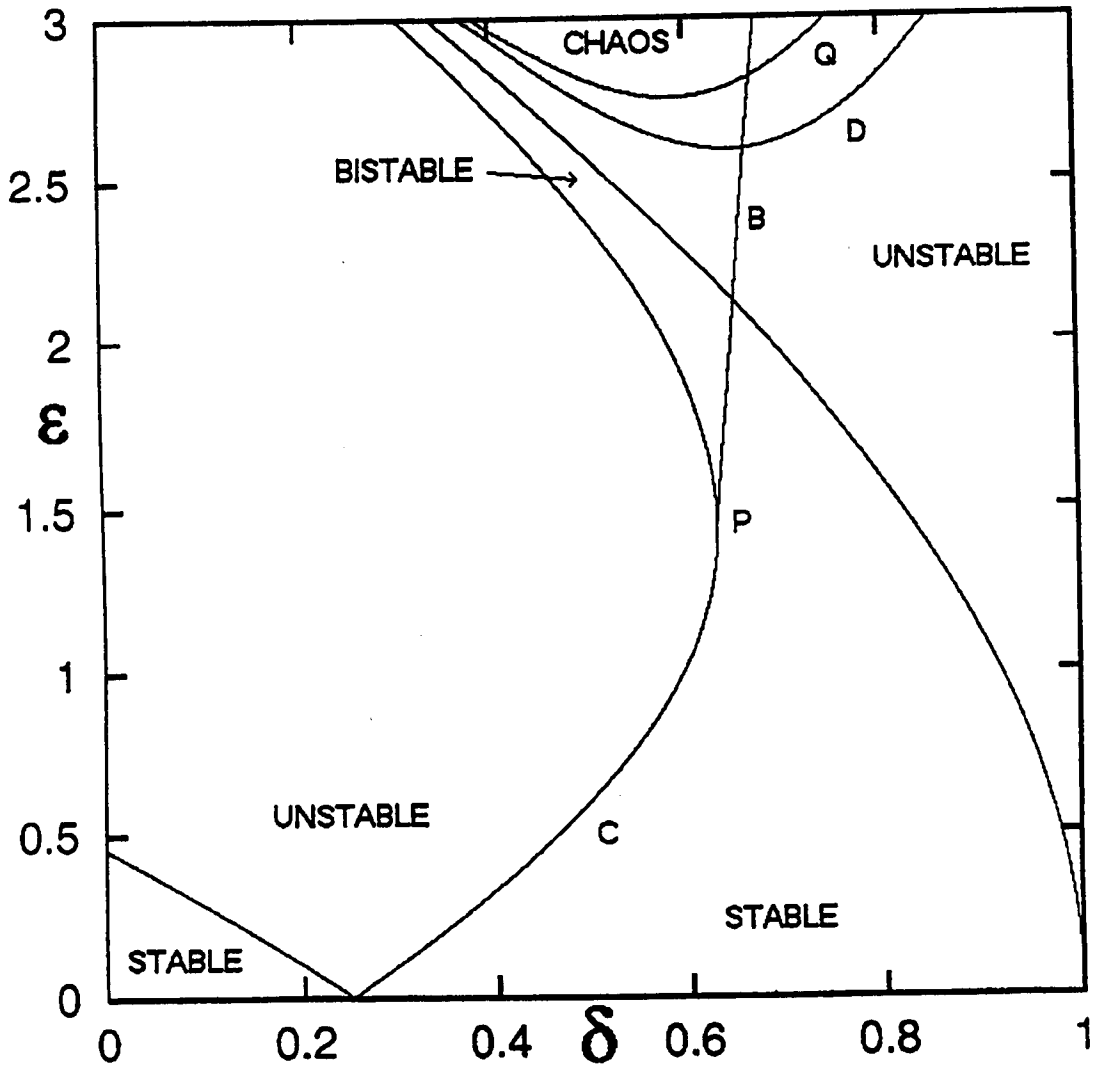

Figure 3. Nonlinear dynamics of eq.(2). Stability of the rest solution $x = 0$ is denoted by "STABLE". Regions marked "UNSTABLE" correspond to unstable rest solution but stable periodic motion. Region marked "BISTABLE" contains both stable rest solution and stable periodic motion. Period-doubling occurs along curve D, and period-quadrupling occurs along curve Q. On curve B́ the system exhibits a secondary bifurcation which can be described as a saddle-node of limit cycles. See text.

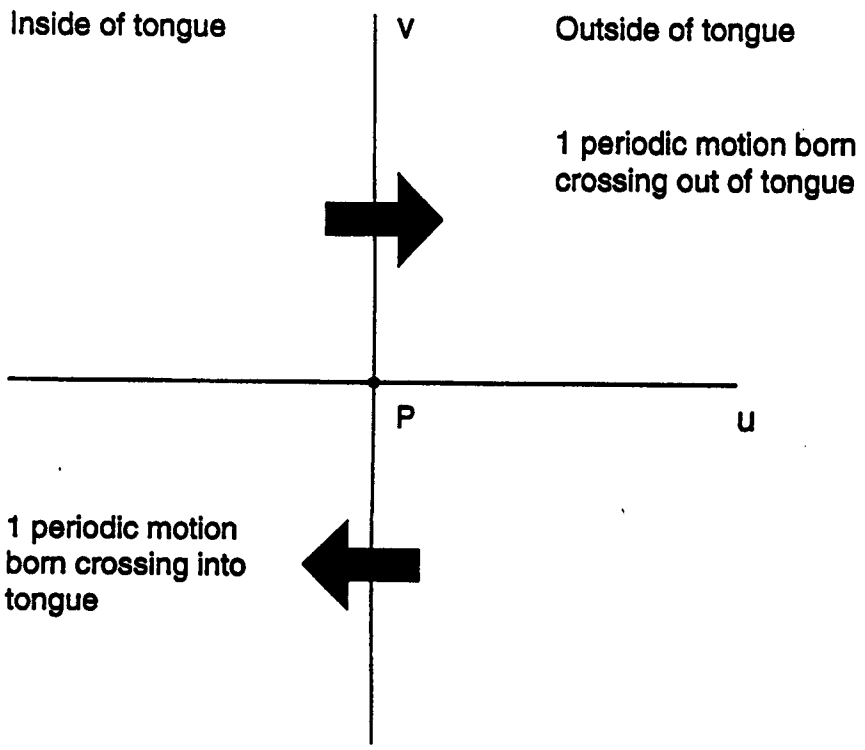

Figure 4. Schematic diagram of bifurcations of the transition curve in the $u - v$ plane. The v–axis corresponds to the transition curve.

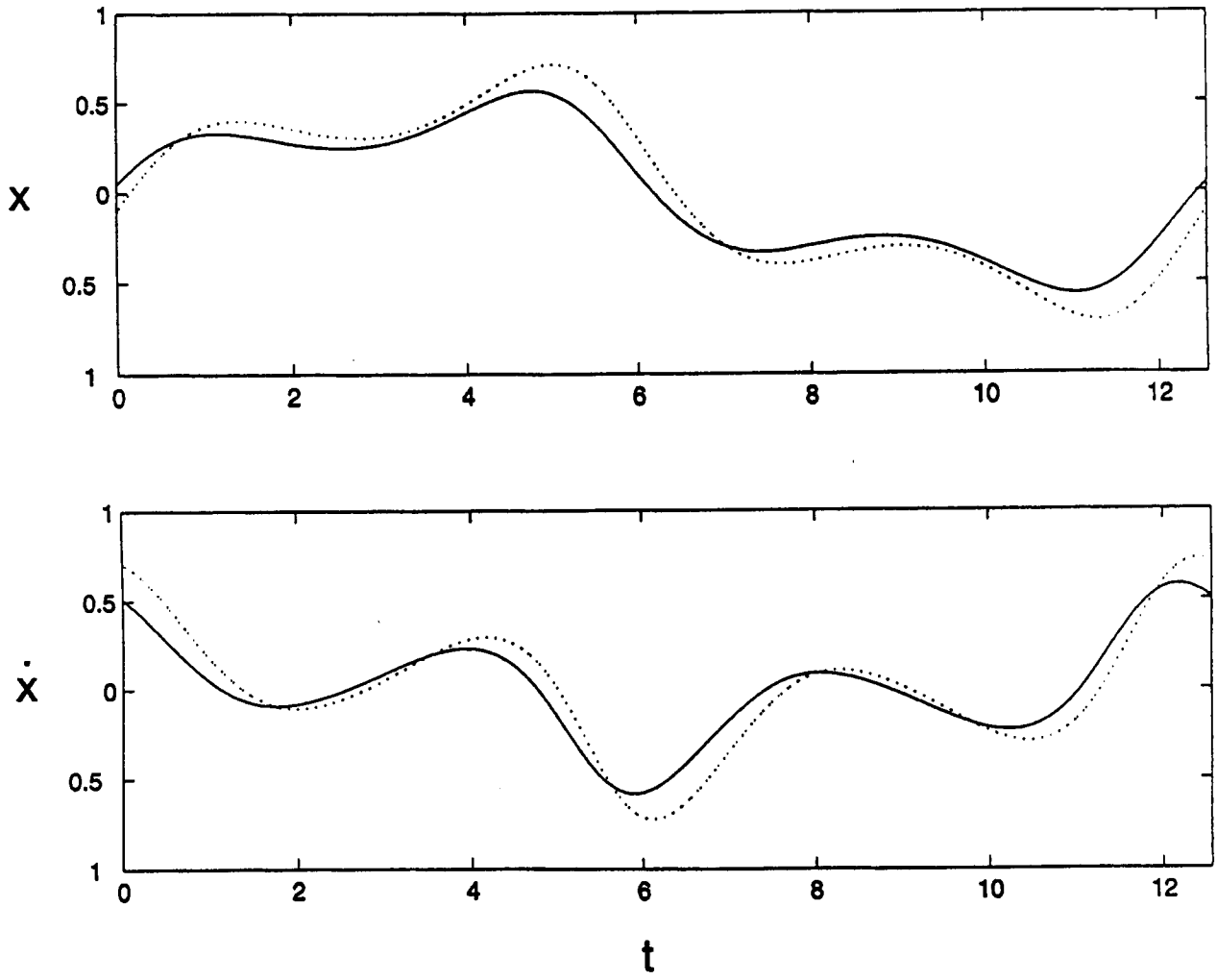

Figure 5. Comparison of numerical and perturbation approximation of periodic orbit above point P and outside the transition curve. Numerical integration is solid, perturbation approximation is dotted. $\delta = 0.631$ and $\epsilon = 1.47$.